eppendorf

Impress Yourself

The new Eppendorf Cell Culture Consumables

The all new line of Eppendorf Cell Culture Consumables will truly delight your cells. The outstanding design, reliability and purity is based on more than 50 years of experience. Products created by experts, developed for perfectionists. Impress yourself!

> Unsurpassed quality, clarity, purity and sterility, providing reliable cell culture conditions
> Significantly improved design for more safety and consistency
> Maximum safety and confidence during storage and transportation

ccc.eppendorf.com • 800-645-3050

STEM CELLS

TISSUE-SPECIFIC STEM CELLS

Serially Transplanted Nonpericytic CD146$^-$ Adipose Stromal/Stem Cells in Silk Bioscaffolds Regenerate Adipose Tissue In Vivo

TRIVIA P. FRAZIER,[a] ANNIE BOWLES,[a] STEPHEN LEE,[b] ROSALYN ABBOTT,[c,d] HUGH A. TUCKER,[a] DAVID KAPLAN,[c,d] MEI WANG,[b] AMY STRONG,[a] QUINCY BROWN,[b] JIBAO HE,[b] BRUCE A. BUNNELL,[a,e] JEFFREY M. GIMBLE[b,f,g,h,i]

Key Words. Adipose stem cells • Adult stem cells • CD34+ • Differentiation • Fluorescence-activated cell sorter • Progenitor cells • Stem cell transplantation • Stromal cells

[a]Center for Stem Cell Research and Regenerative Medicine, [e]Department of Pharmacology, [f]Department of Medicine, [g]Department of Structural and Cellular Biology, and [h]Department of Surgery, Tulane University School of Medicine, New Orleans, Louisiana, USA; [b]Department of Biomedical Engineering, Tulane University, New Orleans, Louisiana, USA; [c]Department of Biomedical Engineering and [d]Department of Chemical Engineering, Tufts University, New Orleans, Louisiana, USA; [i]LaCell, LLC., New Orleans Bio-innovation Center, New Orleans, Louisiana, USA

Correspondence: Jeffrey M. Gimble, M.D., Ph.D, LaCell LLC, 1441 Canal Street, New Orleans LA 70112. Telephone: 504-598-5246; Fax: 504-988-7710; e-mail: jgimble@tulane.edu

Received March 23, 2015; accepted for publication October 29, 2015; first published online in STEM CELLS *EXPRESS* February 11, 2016.

1066-5099/2016/$30.00/0

http://dx.doi.org/10.1002/stem.2325

ABSTRACT

Progenitors derived from the stromal vascular fraction (SVF) of white adipose tissue (WAT) possess the ability to form clonal populations and differentiate along multiple lineage pathways. However, the literature continues to vacillate between defining adipocyte progenitors as "stromal" or "stem" cells. Recent studies have demonstrated that a nonpericytic subpopulation of adipose stromal cells, which possess the phenotype, CD45$^-$/CD31$^-$/CD146$^-$/CD34$^+$, are mesenchymal, and suggest this may be an endogenous progenitor subpopulation within adipose tissue. We hypothesized that an adipose progenitor could be sorted based on the expression of CD146, CD34, and/or CD29 and when implanted in vivo these cells can persist, proliferate, and regenerate a functional fat pad over serial transplants. SVF cells and culture expanded adipose stromal/stem cells (ASC) ubiquitously expressing the green fluorescent protein transgene (GFP-Tg) were fractionated by flow cytometry. Both freshly isolated SVF and culture expanded ASC were seeded in three-dimensional silk scaffolds, implanted subcutaneously in wild-type hosts, and serially transplanted. Six-week WAT constructs were removed and evaluated for the presence of GFP-Tg adipocytes and stem cells. Flow cytometry, quantitative polymerase chain reaction, and confocal microscopy demonstrated GFP-Tg cell persistence, proliferation, and expansion, respectively. Glycerol secretion and glucose uptake assays revealed GFP-Tg adipose was metabolically functional. Constructs seeded with GFP-Tg SVF cells or GFP-Tg ASC exhibited higher SVF yields from digested tissue, and higher construct weights, compared to nonseeded controls. Constructs derived from CD146$^-$ CD34$^+$ -enriched GFP-Tg ASC populations exhibited higher hemoglobin saturation, and higher frequency of GFP-Tg cells than unsorted or CD29$^+$ GFP-Tg ASC counterparts. These data demonstrated successful serial transplantation of nonpericytic adipose-derived progenitors that can reconstitute adipose tissue as a solid organ. These findings have the potential to provide new insights regarding the stem cell identity of adipose progenitor cells. STEM CELLS *2016;34:1097–1111*

SIGNIFICANCE STATEMENT

This study addresses the question of whether to identify cells isolated from fat as "stromal" or "stem" cells. Adipose-derived progenitors possess stem-like characteristics of self-renewal, and the ability to form cells of multiple tissues. However, the literature waivers between calling them "stromal" versus "stem" cells. We report on the self-renewal properties of a specific type of adipose progenitor based on its ability to survive, grow, and form fat in mice over repeated cycles into different mice. This will have profound impact on the way we treat adipose progenitors in the laboratory, and how we use them to treat patients.

INTRODUCTION

The term "stem cell" was first introduced by 19th century embryologists to describe the germline lineages and, shortly thereafter, was associated with the development of the hematopoietic system [1]. A true "stem" cell, as demonstrated by the classical adult hematopoietic stem cell (HSC) model, is defined as possessing the ability to differentiate along lineage specific pathways and to self-renew in vivo [1, 2]. Only a decade ago, investigators believed that bone marrow was the only adult tissue site that contained stem cells; however,

multiple studies of adipose tissue have challenged this paradigm. In 2006, the International Society for Cellular Therapy (ISCT) [3] issued a statement regarding the definition of MSC, where the acronym is specifically defined as "multipotent stromal cells" rather than "mesenchymal stem cells" to avoid the use of "stem" as a terminology. Specifically within adipose, in vitro studies have documented the ability to isolate progenitor cells from the stromal vascular fraction (SVF) of human subcutaneous white adipose tissue (WAT). These cells can form clonal populations and differentiate along multiple lineage pathways [3–6]. Adipose-derived progenitors expressed "stem" cell associated surface antigens (CD34) and transcription factors (Oct4, Sox2) [5–7]. While some argue that the progenitors in adipose tissue derive from bone marrow depots as a circulating population [8–10], there is ample data supporting the presence of an endogenous progenitor subpopulation within the adipose tissue itself [11–13]. Multiple studies have attempted to isolate and characterize this progenitor population, and a subset have reported data suggesting that these cells are a nonpericytic subpopulation within the SVF and are associated with a $CD34^+/CD29^+$ $CD146^-$ phenotype. Nevertheless, the literature continues to waver between defining adipocyte progenitors as "stromal" versus "stem" cells [3, 4, 14]. Over the past decade, there has been a good deal of controversy at the scientific and public level associating the term "stem" exclusively with pluripotent cells derived from embryos, rather than with cells from adult tissues. Thus, the question remains whether the adipose-derived progenitor cell is a "stromal" or "stem" cell.

The distinction between adipose progenitor cells as a "stromal" cell versus a "stem" cell is multifaceted and has considerable implications at the basic science, clinical, and translational levels. For example, a growing number of reconstructive surgeons are using autologous SVF cells isolated from adipose tissue as an "off label" product for various purposes in the operating room [15–17]. Data from multiple studies supports the premise that multipotent stromal cells contained within the SVF accelerate regeneration of injured tissue through their regulation and release of cytokine/chemokine growth factors post implantation [18–20]. Based on this evidence, cardiologists, neurologists and vascular surgeons are seeking to exploit the angiogenic cytokine secretory capacity of adipose-derived cells to treat myocardial infarction [21–24], stroke [25–27], and peripheral limb ischemia [28–32].

Furthermore, recent studies have demonstrated that a specific, nonpericytic subpopulation of adipose stromal cells within the SVF, which possess the phenotype, $CD45^-/CD31^-/CD146^-/CD34^+$, are highly mesenchymal in phenotype [$(94.4 \pm 3.2)\%$ $CD73^+/CD105^+$, $(95.5 \pm 1.2)\%$ $CD90^+$] [12]. These studies also suggest that a relationship exists between pericytes and this nonpericytic SVF subpopulation, with the $CD45^-/CD31^-/CD146^-/CD34^+$ GFP-Tg ASC being the most mesenchymal of SVF cells [12, 33]. To our knowledge, no studies have reported on the regenerative capacity of a flow sorted, nonpericytic ($CD146^-/CD34^+$) SVF subpopulation in a serial transplantation model that is similar to the original HSC model.

The aim of this study was to investigate the self-renewal properties of a nonpericytic SVF subpopulation, and thereby determine the importance of stem cell self-renewal as a contributory mechanism for SVF cell and adipose stromal/stem cells (ASC) function in vivo. Due to the unique association of CD146 with pericytes, and CD34 with ASC (as opposed to bone marrow-derived mesenchymal stromal cells, BMSC) as well as with hematopoietic stem and progenitor cells, $CD146^-$, $CD34^+$ phenotypic expression was chosen for analysis of "stemness" within the study. In comparison, CD29, or β1 integrin, is an abundant surface antigen that has been associated with both ASC and BMSC functionality. Thus, we hypothesized that a labeled nonpericytic adipose progenitor could be sorted based on the expression of CD146, CD34, and/or CD29 and, when placed in vivo, could persist, proliferate, and generate a functional fat pad over serial transplants. The novelty of this study lies in the combination of transgenic labeled cell populations with three-dimensional (3D) tissue engineered constructs for serial transplantation of adipose depots. Since "serial transplantation" has been a critical "gold standard" for the definition of HSCs and bone marrow transplantation for nearly five decades, the concept of serial transplantation of stem cells reconstituting adipose tissue as a solid organ has the potential to provide new insights regarding the stem cell identity of adipose progenitor cells.

Materials and Methods

Materials

Unless otherwise specified, all antibodies were purchased from (eBioscience, San Diego, CA, www.ebioscience.com/) or (Biolegend, San Diego, CA, www.biolegend.com) and all chemicals were purchased from (Sigma-Aldrich, St. Louis, MO, http://www.sigmaaldrich.com/united-states.html) or (Fisher Scientific, Norcross, GA, https://www.fishersci.com/).

Mice

Animal studies were performed under the veterinary supervision of the Department of Comparative Medicine of the Tulane University School of Medicine under a protocol reviewed and approved by the Institutional Animal Care and Use Committee in accordance with federal, state, and National Institute of Health policies and regulations. SVF cells and ASC were isolated from 8 to 12 week male C57BL/6-Tg (UBC-GFP) 30cha/J mice (human ubiquitin C promoter driven green fluorescent protein (GFP) transgene, Jackson Laboratory, Bar Harbor, ME, https://www.jax.org) according to published methods [12]. GFP transgene (GFP-Tg) ASC retain expression of the GFP transgene upon isolation and in vitro expansion out to at least 10 passages, and display a cell doubling time of between 2 and 2.5 days. For initial characterization, cells were examined for expression of markers CD11b (Mac-1α; Integrin alpha M), CD29 (β1 integrin), CD34 (mucosialin), CD45 (leukocyte common antigen; Ly5), CD90 (Thy-1), and Sca-1 (stem cell antigen 1; Ly6A/E).

Adipose Tissue Harvest and SVF Cell Preparation

Subcutaneous inguinal white adipose tissue (iWAT) from 8 to 12 week male C57BL/6-Tg (UBC-GFP) 30cha/J mice was isolated, minced, and digested with collagenase for 60 minutes according to a published protocol from our laboratory [32]. Briefly, the iWAT SVF pellets were collected by centrifugation, washed in phosphate buffered saline (PBS), filtered through a 70 μm mesh (Millipore, Billerica, MA, http://www.

emdmillipore.com/), and the SVF cell concentrations determined by automated Cell Countess (Invitrogen, Carlsbad, CA, https://www.thermofisher.com/us/en/home/brands/invitrogen.html) count. The 1° SVF cells were suspended in Stromal Medium (DMEM/F-12 Ham's, 10% FBS [Hyclone, Logan, UT, http://www.hyclone.com], 100 U penicillin/ 100 g streptomycin/0.25 g fungizone) at a density of 0.156 ml of tissue digest per square centimeter of surface area for expansion and culture to get GFP-Tg ASC, or resuspended at a final concentration of 1×10^6 nucleated cells per milliliter in PBS, in preparation for staining.

SVF Cell Initial Immunophenotype and Subfractionation

Cell suspensions were incubated with antibodies against the cell surface antigens listed in Supporting Information Table at room temperature (RT) for 30 minutes, protected from light. After two washes with PBS, flow cytometric analysis was performed using a Beckman-Coulter Galios flow cytometer (BD Biosciences, San Jose, CA, www.bdbiosciences.com). The immunophenotype and relative subpopulations within the GFP-Tg SVF cells were determined out to passage 2 of plastic adherent culture using fluorochrome-conjugated monoclonal antibodies detecting the following panel of endothelial, hematopoietic, mesenchymal, and stem cell-associated antigens using the scheme provided in Supporting Information Table.

SVF Cell Selection

Two studies were performed that utilized GFP-Tg cells from GFP-Tg C57BL/6 mice (see Methods Figure S1). These include serial transplantation of GFP-Tg unfractionated SVF cells, and serial transplantation of live-cell sorted, culture expanded GFP-Tg ASC subpopulations. For the first study, GFP-Tg SVF cells were selected by flow sorting for the GFP-Tg population, and unfractionated GFP-Tg SVF cells were immediately loaded onto silk scaffolds for GFP-Tg SVF serial transplantation in non-GFP-Tg mice. For the second study, the GFP-Tg $CD146^-$ SVF subpopulation was selected and either plated as: (a) unfractionated controls, or sorted based on (b) CD29 positivity, and (c) CD34 positivity. The culture-expanded populations (a–c) were immunophenotyped, and loaded onto silk scaffolds for GFP-Tg ASC serial transplantation (ASC serial transplantation studies; see HexaFluoroIsoPropanol Silk Scaffold Loading, Culture, and Implantation below).

ASC Culture Expansion

Live cell sorting of GFP-Tg 1° SVF cells was performed using a BD Biosciences fluorescence-activated cell sorter (FACS) Beckman-Coulter Galios flow cytometer with two lasers and eight detectors running Galios acquisition software (BD Biosciences, San Jose, CA). All selected fluorochromes remained compatible with the continued use of the transgenic GFP for cell sorting purposes. Lineage depletion was performed using a cocktail of eFluor-conjugated antibodies detecting murine (mu) CD3, CD45R, CD116, LyG6, Ter-119 (eBioscience; 88-7772). Live SVF cell selection was performed with APC conjugated anti-muCD29 (17-0291) and PE conjugated anti-muCD34 (56-0341). ASC were isolated following plastic adherent culture expansion and using phenotypic and functional criterion established by International Federation of Adipose Therapeutics (IFATS) and the ISCT [3]. Briefly, passage 0° (P0) ASCs were subjected to trypsinization with 5 ml 0.25% trypsin (Life Technologies, Grand Isle, NY) for 5 minutes. Trypsin digestion was stopped by the addition of an equal amount of ASC culture medium. P0 ASCs were counted using trypan blue dye exclusion, and passaged in new T175 flasks at a density of 0.4×10^3 cells per square centimeter. Cells were cultures until they reached 70% confluency. Populations were culture expanded to P2 as (a) unfractionated as controls or subfractionated into (b) a $CD29^+$ enriched population (Lin^- $CD29^+$ $CD146^-$) or (c) a $CD34^+$ enriched population (Lin^- $CD34^+$ $CD146^-$). The (a) unfractionated controls, (b) $CD29^+$ enriched ASC populations, and (c) $CD34^+$ enriched ASC populations were individually seeded in flasks and culture expanded according to our published and validated methods [34]. After sorting for CD29, $95.05 \pm 2\%$ of the cells expressed CD29 and GFP. These SVF subpopulations were immediately plated, expanded, and passaged in order to get a sizeable population for seeding. Please note that the cells ($CD29^+$ and $CD34^+$ subpopulations) were selected separately, and were not sorted based on coexpression of both CD29 and CD34. In addition, the initial CD34 sorted subpopulation ($99.85 \pm 4\%$ positive for both GFP and CD34) included other SVF precursor populations that may coexpress CD34, and would be eliminated during plastic adherent expansion and selection of the adherent ASC populations; therefore, the initial sorted CD34 expression in SVF cells would be higher than that of culture-expanded CD34 selected ASCs, which may lose the expression of the surface marker as a function of the adherence and proliferative processes. At passage 2 (P2), an aliquot of the ASC (1×10^5 ASC) from each SVF fraction was characterized by analytical flow cytometry for GFP positivity and the antigens CD29, CD31, CD34, CD45, CD73, CD90, CD105, CD146, and Sca-1 to monitor changes in profile due to expansion [33]. In parallel, the live P2 GFP-Tg ASC were evaluated for proliferation, colony formation, and adipogenic differentiation in vitro or for implantation studies (see below).

HexaFluoroIsoPropanol Silk Scaffold Loading, Culture, and Implantation

The HexaFluoroIsoPropanol (HFIP) silk scaffolds obtained from the Tissue Engineering Resource Center, (Tufts University, Medford, MA, http://ase.tufts.edu/terc/) University were prewet overnight at 4°C in Stromal Medium (Dulbecco's modified Eagle's-Ham's F-12 medium supplemented with 10% fetal bovine serum and 1% penicillin/streptomycin). The scaffolds were used in studies with unfractionated SVF cells, and with studies using fractionated passage 2 (P2) ASC. For the SVF study, the freshly isolated GFP-Tg iWAT 1° SVF cells were loaded by pipet in two aliquots of 50 μl each containing a total of 2.5×10^5 cells to opposite faces of a cylindrical HFIP silk scaffold as per our published methods [33]. For the ASC study, a sample of freshly isolated GFP-Tg iWAT 1° SVF cells was directly plated (unfractionated), or sorted based on $CD146^-$ $CD29^+$ or $CD146^-/CD34^+$ expression. The subfractions were plated and cultured until P2. The P2 ASC derived from unfractionated SVF controls, $CD146^-$ $CD29^+$ enriched populations, and $CD146^-$ $CD34^+$ enriched populations were loaded by pipet in two aliquots of 50 μl each containing a total of 2.5×10^5 cells to opposite faces of a cylindrical HFIP silk scaffold.

For both studies, the scaffolds were transferred to a humidified 37°C, 5% CO_2 incubator, and rotated every 15

minutes over a 2-hour period. Following the addition of 5 ml of Stromal Medium, each scaffold was immediately implanted into 8-week male nontransgenic C57Bl/6 mice. A set of representative scaffolds (1° SVF cell or cultured ASC population) were retained, fresh frozen in optimal cutting temperature compound (OCT), and stored for use as positive controls. The remaining individual scaffolds loaded with SVF cells or ASC ($n = 20$ for each subpopulation) were implanted bilaterally into a dorsal subcutaneous pouch created in C57Bl/6 mice according to standard veterinary practices under an approved IACUC protocol (Protocol #4302). Each transplanted mouse was implanted with a randomized combination of empty scaffolds (control), those seeded with SVF cells, or P2 ASC that were unfractionated controls, $CD29^+$ enriched population ($CD29^+$ $CD146^-$), or $CD34^+$ enriched population ($CD34^+$ $CD146^-$).

Proliferation Assay

Immediately after cell seeding, the relative number of metabolically active stem cells within each seeded scaffold was determined by the AlamarBlue™ assay according to the manufacturer's instructions [35]. Seeded scaffolds were incubated in Stromal Medium supplemented with 10% Alamar Blue reagent for 2 hours at 37°C with 5% CO_2. Aliquots (100 μl) of the culture medium were transferred to 96-well plates and quantified for fluorescence intensity with a microtiter plate reader (Fluostar Optima) using an excitation wavelength of 560 nm and an emission wavelength of 590 nm. Nonseeded scaffolds and tissue culture wells were also maintained in culture medium as above and were analyzed similarly as blank controls to adjust for background fluorescence. Scaffolds were then weighed and the relative cell numbers were calculated as the degree of their relative fluorescence intensity (RFU) per milligram of scaffold wet weight as previously described [35].

Adipogenic Differentiation

Adipogenic differentiation of culture-expanded and scaffold-seeded non-GFP-Tg ASC or GFP-Tg ASC was performed over a 15-day period as previously described [4]. Briefly, cultured ASC were grown in Stromal Medium (Dulbecco's modified Eagle's-Ham's F-12 medium supplemented with 10% fetal bovine serum, and 1% penicillin/streptomycin). ASC were then trypsinized and plated in 24-well plates in ASC culture media at 3×10^4 cells per square centimeter for 24 hours to allow attachment. On day 1 (24 hours after plating), the medium was removed and cells were incubated for 3 days in adipogenic differentiation medium (Dulbecco's modified Eagle's-Ham's F-12 medium supplemented with 10% fetal bovine serum, 15 mM HEPES [pH 7.4], biotin [33 μM], pantothenate [17 μM, Sigma], human recombinant insulin [100 nM, Boehringer Mannheim], dexamethasone [1 μM], 1-methyl-3-isobutylxanthine [IBMX; 0.25 mM], and rosiglitazone [1 μM]). For the remaining 9 days of the adipocyte differentiation maintenance period, the medium was removed every 3 days and replaced with the same medium that did not contain IBMX and rosiglitazone (maintenance medium).

Adipogenesis of Scaffold-Seeded Cells

For scaffold-seeded GFP-Tg SVF cells and GFP-Tg ASC, one day prior to seeding, scaffolds were autoclaved and presoaked in adipogenic medium in 37°C, 5% CO_2, 95% relative humidity. GFP-Tg ASC were then trypsinized and plated loaded onto presoaked scaffolds in ASC adipogenic differentiation media by pipet in two aliquots of 50 μl each containing a total of 2.5×10^5 cells to opposite faces of a cylindrical HFIP silk scaffold as per published methods [33]. The cells were incubated for 3 days in adipogenic differentiation medium (Dulbecco's modified Eagle's-Ham's F-12 medium supplemented with 10% fetal bovine serum, 15 mM HEPES [pH 7.4], biotin [33 μM], pantothenate [17 μM, Sigma], human recombinant insulin [100 nM, Boehringer Mannheim], dexamethasone [1 μM], 1-methyl-3-isobutylxanthine [IBMX; 0.25 mM], and rosiglitazone [1 μM]). For the remaining 9 days of the adipocyte differentiation maintenance period, the medium was removed every 3 days and replaced with the same medium that did not contain IBMX and rosiglitazone (maintenance medium). Similarly, control cultures were maintained in parallel in the absence of adipogenic stimulants. All seeded and nonseeded (control) scaffolds were cultivated in a humidified incubator at 37°C with 5% CO_2. Following the in vitro cultivation period, seeded scaffolds were evaluated for their extent of adipogenesis.

Intracytoplasmic Lipid Quantification

For plastic adherent cultured ASC, lipid formation was assessed by incorporation of Oil-Red-O (ORO) (Sigma-Aldrich) into monolayers of GFP-Tg ASC cultured in adipocyte differentiation medium for 12 days. Quantitation of ORO incorporation was performed as previously described [4]. Briefly, 0.5% (w/v) ORO was prepared in ethanol. Three parts ORO and two parts PBS were then mixed to make a working solution. Monolayers of GFP-Tg ASC cultured in 12-well plates were rinsed three times with PBS and subsequently fixed in 10% (v/v) formalin (Sigma-Aldrich) for 15 minutes. The monolayers were then rinsed three times with PBS and then incubated in ORO working solution for 45 minutes at RT. Following aspiration of unincorporated ORO, monolayers were rinsed four times with PBS. Stained monolayers were visualized with phase contrast microscopy (Eclipse 800, Nikon, Tokyo, Japan, http://www.nikon.com/). Incorporated ORO was extracted by incubating stained monolayers in 100% isopropanol for 10 minutes. The absorbance at 510 nm of each aliquot was then measured using a 96-well plate reader (Fluostar Optima, BMG Labtech, Cary, NC, http://www.bmglabtech.com/).

For scaffold-loaded ASC, accumulated lipid was also visualized using ORO staining. Scaffolds were fixed in 2 M sucrose overnight for histology. The scaffolds were embedded in OCT medium, frozen over dry ice, and stored at −80°C. Frozen scaffolds were then sectioned (7-μm sections) using a cryostat and stained. For ORO staining, frozen sections were fixed in 10% buffered neutral formalin for 15 minutes, and rinsed with distilled water. ORO working solution was placed onto frozen sections and incubated for 20 minutes. Slides were rinsed with distilled water, and counterstained with 4′,6-diamidino-2-phenylindole (DAPI) according to manufacturer's protocol. Stained sections were covered using glass cover slips. Images were taken using phase contrast microscopy.

Serial Transplantation

The transplanted animals were maintained for 6–8 weeks, euthanized, and the scaffolds were removed using aseptic dissection techniques. Prior in vivo studies have demonstrated

that 4–6 weeks is a sufficient period to allow for human ASC adipogenesis in transplanted silk scaffolds [33]. We observed a surge in GFP-Tg cell expansion and differentiation by confocal microscopy following 6 weeks. Therefore, our studies were carried out to week 6. Sets of $n = 2$ scaffolds were fresh frozen in OCT for microscopic analyses. The remaining $n = 18$ scaffolds were subjected to collagenase digestion for 1 hour in PBS supplemented with 0.1% collagenase type I (Worthington Biochemicals, Brunswich, Lakewood, NJ, http://www.worthington-biochem.com), 1% bovine serum albumin, and 2 mM $CaCl_2$ for 60 minutes at 37°C with intermittent shaking. The 2° (secondary implanted) SVF cells were isolated as described above, under HFIP Silk Scaffold.

Loading, Culture, and Implantation

The frequency of GFP-Tg cells in the 2° SVF as well as their expression of associated antigens (panel of monoclonal antibodies (mAbs) above) were determined by analytical flow cytometry using a sample of each grouping. The remaining sorted 2° SVF cells from the original cohorts were loaded onto freshly prepared HFIP silk scaffolds by repeating the same process above. After incubation, the scaffolds were loaded with the 2° SVF cells and were implanted bilaterally into C57Bl/6 mice for a 6-week period. At that time, the scaffold harvest and analysis was repeated to yield a 3° SVF cell population. Due to cell harvest constraints, the scaffold harvest and analysis was terminated following 3° SVF cell populations, and 2° ASC populations. As a positive control, intact inguinal depots from C57Bl/6 (UBC-GFP) mice were serially transplanted to congenic wild-type recipients for equivalent periods of time. Additionally, insulin sensitivity within the removed silk scaffold constructs was determined using our published in vitro glucose uptake and lipolysis assays to insure functionality [35]. It should be noted that for the present study time of engraftment was measured between the date of surgical implantation of the scaffold (with or without cells) and the date when it was surgically removed from the animal. For negative control groups, tissue was harvested from age and gender compatible non-GFP-Tg C57BL6 mice.

Hemoglobin Saturation Measurement

The Zenascope PC1 spectrometer (Zenalux, Durham NC, http://www.zenalux.com) employs a broadband halogen light source (probe) to illuminate the target tissue. The Zenascope allows measurements of protein levels in live animals, in the absence of invasive techniques. A bifurcated fiber optic probe with stainless steel jacketing and terminating in a 0.25″ diameter stainless steel rigid common end is applied to the surface of the tissue, delivers light to the target tissue and collects the reflected optical signal, and the optical properties (wavelength-dependent absorption and scattering coefficients) of the tissue are quantitatively extracted from the measured reflectance spectra over the wavelength range 500–650 nm. From the extracted absorption coefficient, the portable and standardized measurement hardware achieves rapid, real-time quantitative analysis of oxyhemoglobin (HbO_2), deoxyhemoglobin (dHb), total hemoglobin concentration (Hb, defined as $HbO_2 + dHb$), and hemoglobin oxygen saturation (sO_2, defined as the ratio HbO_2/Hb). The optical reduced scattering coefficient () was also measured and reported by the instrument, which allows measurements of tissue chromophores to be quantified accurately and independently of changes in tissue scattering. Integration times were automatically set by the system software for each measurement to maximize reflectance signal while staying within the linear response range of the detector, and typically ranged from 100 to 200 ms. Reflectance calibration of the probe using a 99% reflectance standard was performed prior to all experiments and periodically during the procedures.

ImageJ Explant Analyses

For reporting on ASC or SVF enhancement engraftment time, three representative images of whole explants that were removed from each cohort were converted to TIF files and exported to ImageJ for analyses. Images from unseeded scaffold explants (control) were quantified using (ImageJ Version 1.46 software, NIH). Pixel values were from the entire tissue explant, not sectioned images. Threshold values were established from subtracting background pixel count using the control. Relative mean pixel counts from groups of tissue sections were averaged and the standard deviation was calculated.

Cryo-Scanning Electron Microscopy

Cryo-scanning electron microscopy was conducted on scaffolds that were seeded with GFP-Tg ASC following 24-hour cell culture. Cryo-SEM structure research was done with Gatan 2500 alto Cryo-system and Hitachi S-4800 scanning electron microscopy (SEM). The tissue was cut to $7 \times 5 \times 5$ (mm) and laid about 5 mm high above a cryogenic SEM sample holder surface, clamped and glued into the holder, and then frozen in slushed liquid nitrogen at approximately −210°C for about 30 seconds. The frozen tissue was transferred in vacuum to the prechamber attached to the SEM and then fractured and sublimed for 5 minutes at −95°C. After coating 88 seconds at −130°C with Pt/Pd, the sample was moved to the SEM and observed at 3kV at −130°C.

Histochemistry

Fresh frozen tissue samples were sectioned, stained with a lipophilic fluorescent dye (Bodipy), and evaluated by confocal fluorescent microscopy for the colocalization of GFP and lipid signals.

Quantitative Polymerase Chain Reaction (qPCR) for GFP Gene Expression

Total DNA was isolated from removed tissue engineered fat pads or positive or negative controls using the Qiagen FFPE tissue prep Mini Kit (Qiagen Inc., Valencia, CA, http://www.qiagen.com) according to the manufacturer's specifications. Polymerase chain reactions were performed with approximately 500 ng of total DNA using the SYBR green real-time PCR DNA binding dye. Reaction mix was incubated with Oligonucleotide primer sets specific for GFP (forward: 5′-TCGCCTACCAGCTCATGCATAACA-3′; reverse: 5′-TGAAGCTCTTCCAGGTGTCAACGA-3′) in a real-time thermal detection system (Bio-Rad Laboratories, Hercules, CA, http://www.bio-rad.com). All results were normalized relative to glyceraldehyde 3′ phosphate dehydrogenase (GAPDH) expression control.

Statistics

All studies were repeated at least in triplicate and values are reported as the mean ± standard deviation (SD). Individual

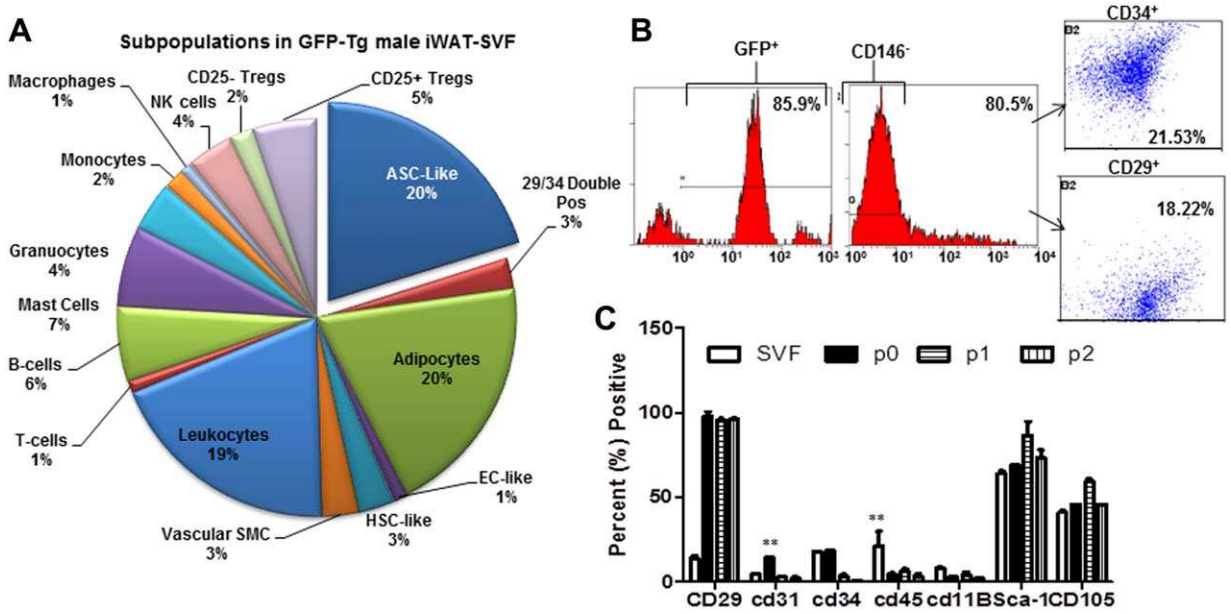

Figure 1. Characterization of cells used in the study. **(A)**: Pie chart of subpopulations within GFP-Tg SVF cells that were utilized for SVF serial transplantation studies. **(B)**: Sorting and enrichment of $CD146^-$ $CD29^+$, and $CD146^-$ $CD34^+$ subpopulations that were culture expanded to P2 ASC for GFP-Tg ASC serial transplantation studies. **(C)**: Immunophenotype of GFP-Tg SVF cells and culture-expanded GFP-Tg ASC, until passage 2 (P2). All experiments were repeated in triplicate; sample size, $n = 3$ per replicate. Values reported as mean $\pm$ standard deviation ($\mu \pm$ SD); *$p < .05$, ** $p < .01$; ***$p < .001$. Abbreviations: ASC, adipose stromal/stem cells; EC, Endothelial cell; GFP-Tg, green fluorescent protein transgene; HSC, hematopoietic stem cell; NK, Natural killer cell; SMC, smooth muscle cell; SVF, stromal vascular fraction.

pairs were compared using the student *T* test while larger groups were analyzed by Analysis of Variance. Findings were defined as significant with minimum p values $\leq .05$.

Results

Isolation and Characterization of Cells Utilized

Figure 1A provides the representative subpopulations of cells detected within GFP-SVF of iWAT isolated from 8 to 12 week male mice. Initial SVF yields averaged $3–5 \times 10^5$ 1° (primary) SVF cells per milliliter of adipose tissue. This is similar to reported values in the literature [33]. The three largest subpopulations based on surface immunophenotype (Supporting Information Table) were the preadipocytes, ($24.7 \pm 6.9\%$; $CD14^-$, $CD36^+$), the ASC-like ($20 \pm 10.7\%$; $CD146^-$, $CD34^+$, $CD90^+$), and the leukocytes ($19.4 \pm 9.7\%$; $CD34^-$, $CD45^+$). Of note, the pelleted SVF cell population excludes floating mature adipocytes (estimated to be about 30% of the total population) due to the process of collagenase type I tissue digestion and isolation by differential centrifugation. The initial SVF fraction was first sorted for the $CD146^-$ subpopulation ($80.5 \pm 5\%$). This served as the initial cohort of fractionated SVF cells. Other cohorts were selected based on sorting for CD34 and CD29 surface antigen expression: (b) $CD29^+$ ($18.2 \pm 8.5\%$ of the $CD146^-$ population), and (c) $CD34^+$ ($21.4 \pm 12.8\%$ of the $CD146^-$ population) SVF cells. The flow cytometry sorting protocol is given in Figure 2. Characteristics of these cohorts [(a) total $CD146^-$ SVF cells, (b) $CD146^-$, $CD29^+$ enriched cells, and (c) $CD146^-$, $CD34^+$ enriched cells] were determined based on immunophenotype of plastic adherent cell culture, proliferation, colony formation, and adipogenic potential out to passage 2 (P2). Similar to other published reports, stromal markers (CD29) increased in expression, and endothelial (CD31, CD45) and hematopoietic markers (CD34, CD11b) decreased in expression over passage. Sca-1 expression averaged $61.6 \pm 10.7\%$ within unsorted SVF populations and increased over passage (Fig. 2A). CD29 and CD34 enrichment resulted in lower Sca-1 expression (CD29; $13.8 \pm 2.4\%$, CD34, $13.7 \pm 0.9\%$). $CD34^+$ enriched subpopulations exhibited significantly higher proliferative and adipogenic potential than $CD29^+$ enriched subpopulations (Fig. 2B). Further, $CD29^+$ subpopulations had slower doubling times and lower intracytoplasmic lipid accumulation than the unsorted populations (Fig. 2C, 2D).

SVF and ASC Seeding on Scaffolds

GFP-ASC in vitro seeding and proliferative properties were investigated following seeding on HFIP-based silk scaffolds. Confocal microscopy was performed on seeded and unseeded control scaffolds after 24 hours of incubation (Supporting Information Fig. 2A). GFP detection and Alamar Blue staining revealed a preference of cell localization on the edges of the silk scaffold honeycomb-like structures (Supporting Information Fig. 2B, bright field and Supporting Information Fig. 2D, scanning electron microscopy). Cells remained on these edges, commenced differentiation (Supporting Information Fig. 2C) and proliferation (Supporting Information Fig. 2D, 2E). Quantitation of Alamar Blue (Supporting Information Fig. 2D) cytosolic and DAPI (Supporting Information Fig. 2E) nuclear positivity revealed the cells were present 2 hours postseeding (18 hours; 16 ± 2 cells; 2 hours, 11 ± 8 cells; Supporting Information Fig. 2E), but adhered to the scaffold and exhibited

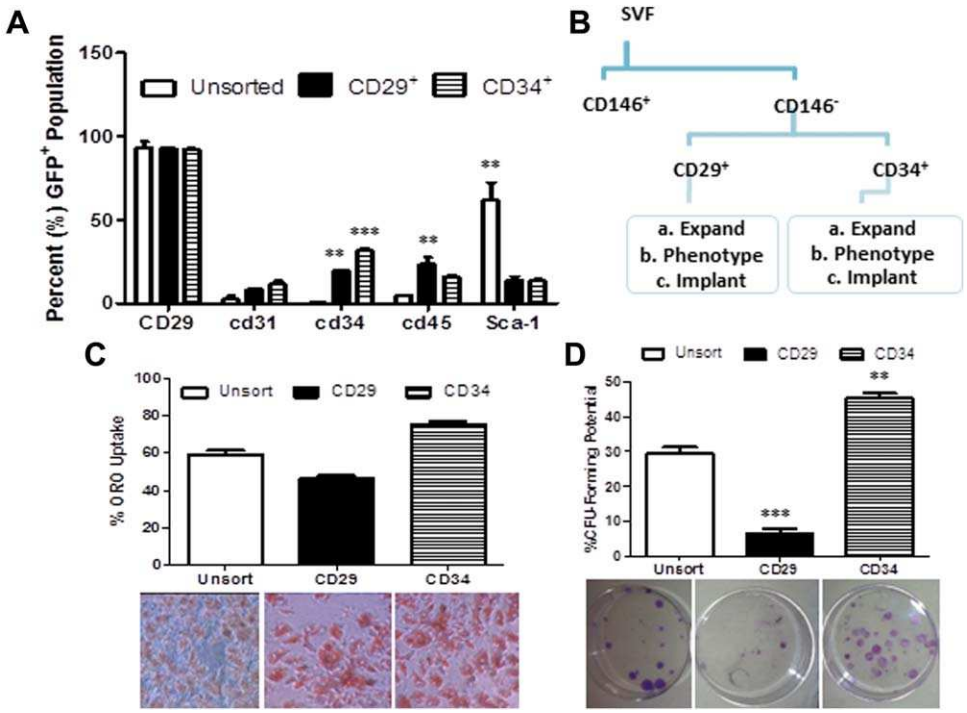

Figure 2. Comparison of CD29-enriched and CD34-enriched green fluorescent protein transgene (GFP-Tg) ASC. **(A)**: Immunophenotype of $CD146^-$ $CD29^+$, and $CD146^-$ $CD34^+$ sorted GFP-Tg ASC subpopulations. Immunophenotypes were based on expression of CD29, CD31, CD34, CD45, CD11B, Sca-1, and CD105 surface antigens. **(C)**: Adipogenic differentiation, and **(D)** colony formation assays of unfractionated GFP-Tg ASC, $CD146^-$ $CD29^+$ GFP-Tg ASC, and $CD146^-$ $CD34^+$ GFP-Tg ASC. All experiments were repeated in triplicate; sample size, $n = 3$ per replicate. Values reported as mean ± standard deviation ($\mu \pm SD$); $^*p < .05$, $^{**}p < .01$; $^{***}p < .001$. Abbreviations: ASC, adipose stromal/stem cells; GFP, green fluorescent protein; SVF, stromal vascular fraction.

measurable metabolic activity by RFU 18 hours postseeding (18 hours, 36 RFU; 2 hours, 0.001 RFU; Supporting Information Fig. 2E).

SVF Cells Enhance Engraftment and Generate Adipose In Vivo

Unfractionated SVF cells were monitored for growth and adipogenesis using a 6-week time course. Photographic analyses revealed that the presence of SVF cells accelerated engraftment by week 1(Fig. 3A). Measurements of percent hemoglobin saturation (%Hb; Fig. 3B) also supported the observed SVF cell-mediated enhanced vascularization. It should be noted that hemoglobin measurements were taken on the skin surface of live mice, and that the measurement of saturation assesses all tissues, not simply the arterial blood supply. By week 2 and beyond, no significant difference in engraftment was observed, both visually and by quantification of explant images using ImageJ (Fig. 3C). This supported published data suggesting the vascular and supportive nature of the scaffolds to promote adipogenesis in vivo. Measurements of scaffold mass (Fig. 3D) and total SVF recovered (Fig. 3E) from seeded scaffolds were significantly higher than unseeded controls during week 1. SVF cell count and scaffold mass reached a maximum at week 2, and decreased by week 4 (Panels 3d, 3e).

Unsorted GFP-SVF Cells Detected Following Serial Transplantation

Weekly detection of unsorted GFP-SVF within initial implants from weeks one to six (Fig. 4A) revealed that GFP-SVF cells were not only persisting within scaffolds, but also proliferating and differentiating as early as week 1 following implantation. Confocal microscopy images are displayed for weeks 1, 4, 5, and 6 of initial SVF explants (Fig. 4A). GFP-Tg SVF cells were detected within explants from initial cohorts (T_0 implants), as well as initial serial (T_1 implants) and secondary serial (T_2 implants; Fig. 4B) transplants. Flow cytometry-based detection of GFP-Tg SVF cells was consistent with confocal microscopy observations (Fig. 4C). Initial implants resulted in 19% GFP antigen positivity via flow cytometry at week 4 while T_1 and T_2 implants resulted in 16.2% and 13.1% GFP positivity, respectively, at the same time points relative to implantation (Fig. 4C). Quantification of GFP, BODIPY lipophilic dye staining (to demonstrate the adipogenic nature of the constructs), and the nuclear DAPI stain colocalization was performed using ImageJ. Quantification demonstrated a 50% increase in GFP-Tg SVF cell percentage by week 6 following T_0 implants, compared to week 1 (Fig. 4D). It is important to note that the flow cytometry data reported in Figure 4D is conducted on the SVF cells that have been isolated from the tissue reported in Figure 4C. Adipose tissue contains mature adipocytes and other cells that would not survive the tissue digestion procedure, and would not be reflected in the flow cytometry numbers. Figure 4D, therefore, does not reflect all cells in the tissue sample. GFP expression within removed explants was further investigated based on protein and DNA levels via flow cytometry and qPCR, respectively (Fig. 4E, 4F). Weekly detection of percent GFP-Tg cells via flow cytometry revealed an increase in expression from 3.8% in week 2 to 16% by week

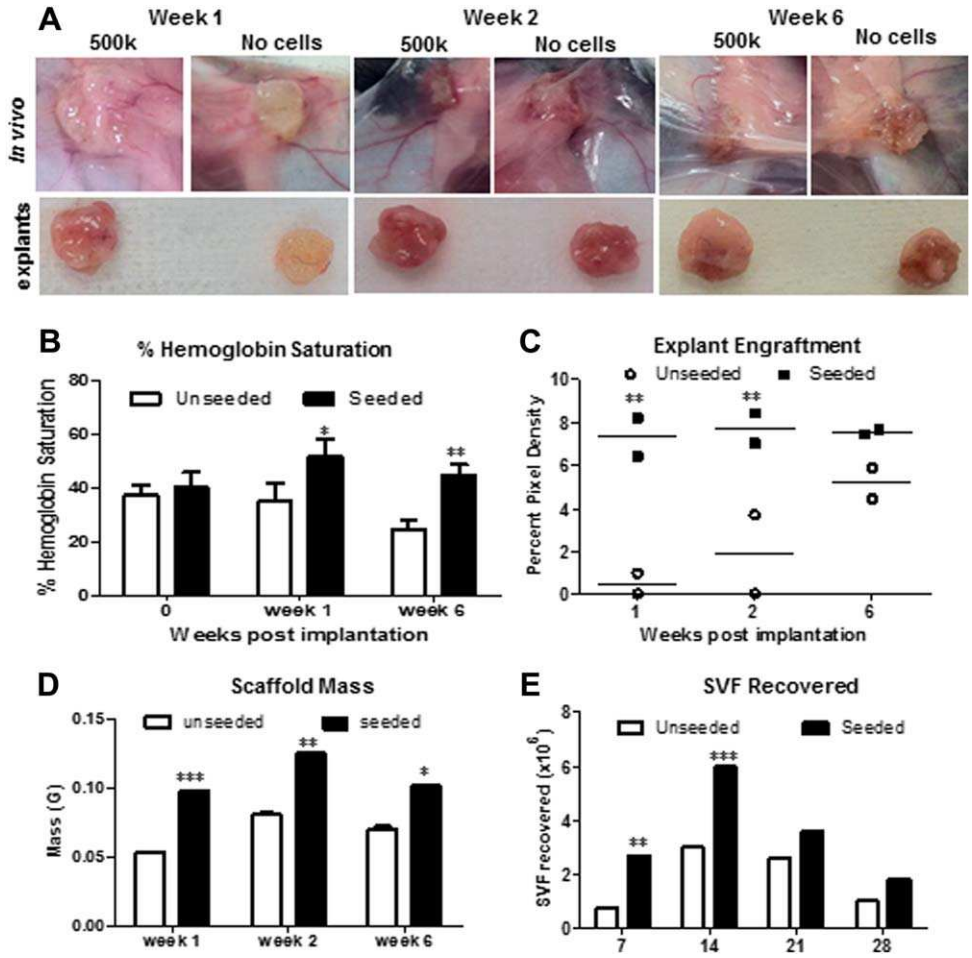

Figure 3. Weekly progression of tissue engineered fat within and surrounding green fluorescent protein transgene (GFP-Tg) SVF cell implants in mice. **(A)**: Scaffolds were implanted with no cells, or with 500k GFP-Tg SVF cells in silk scaffolds. Scaffolds were removed following 1 week, 2 weeks, or 6 weeks of implantation. **(B)**: Percent hemoglobin saturation was measured immediately following implantation, and after 1 week and 6 weeks of initial implantation. **(C)**: Quantification of removed scaffold (explant) engraftment via ImageJ analyses of photomicrographs in Fig. 3A; sample size, $n = 6$ per group. **(D)**: Scaffold mass measurements following weeks 1, 2, and 6 of implantation; sample size, $n = 20$. Quantification supports photomicrographs of SVF-mediated engraftment acceleration after 1 week of implantation. **(E)**: Weekly SVF cell quantification correlate with SVF cell persistence and expansion by week 2, and differentiation. Values reported as mean ± standard deviation ($\mu \pm SD$); $^*p < .05$, $^{**}p < .01$; $^{***}p < .001$. Abbreviations: SVF, stromal vascular fraction.

4 following T_0 implants (Fig. 4E). GFP DNA expression was enriched more than 200-fold (unseeded scaffold implants in nontransgenic mice) following T_2 implants (Fig. 4F). The surface immunophenotype of cells from the T_2 implant population was also compared to GFP-Tg controls and unseeded scaffold controls following 6 weeks (Fig. 4G). The T_2 scaffolds displayed 36.3 ± 2.4% GFP positivity, 67.8 ± 4.1% CD29 positivity, and 52.4 ± 2.4% CD45 positivity (Fig. 4G).

CD34-Enriched GFP-Tg ASC Enhance Engraftment and Generate Functional Adipose In Vivo

GFP-Tg SVF cells were isolated and grouped as unfractionated cells, or sorted as $CD146^-$ $CD29^+$ enriched, or $CD146^-$ $CD34^+$ enriched groupings. These cells were culture expanded to P2 GFP-Tg ASC, seeded on silk scaffolds, and implanted into nontransgenic mice until T_0 serial transplant. No visual difference in fat depot size was observed at week 6 of implant removal (Fig. 5A, 5b). Measurements of percent hemoglobin (%Hb) saturation and explant engraftment were investigated. Implants seeded with both CD29- and CD34-enriched GFP-Tg ASC exhibited higher %Hb saturation following 1 week of implantation compared to both unseeded implants and implants seeded with unsorted ASC control (Fig. 5C). Further, CD34-enriched implants exhibited significantly higher %Hb saturation than CD29-enriched implants (Unseeded ASC: control, 37.6 ± 9.9%; CD34-enriched, 68.1 ± 5.3%; CD29-enriched, 45 ± 10.8%; Fig. 5C). This was observed visually and quantitatively using ImageJ software analyses of photomicrographs (Fig. 5D). Measurements of explant mass and mass of the surrounding fat (Fig. 5E) revealed that the engineered constructs originating from CD34-enriched implants were significantly more dense than CD29-enriched and unsorted GFP-Tg ASC, as well as unseeded controls (Fig. 5E). Total SVF recovered (Fig. 5F) from CD34-enriched ASC-seeded scaffolds were also significantly higher than CD29-enriched, unsorted ASC, and unseeded controls during week 1 (Fig. 5F). Further investigation of tissue engineered fat functionality revealed CD34-enriched constructs secreted glycerol levels comparable to unsorted ASC constructs, whereas CD29-enriched constructs secreted significantly lower levels of glycerol (Fig. 5G). No significant

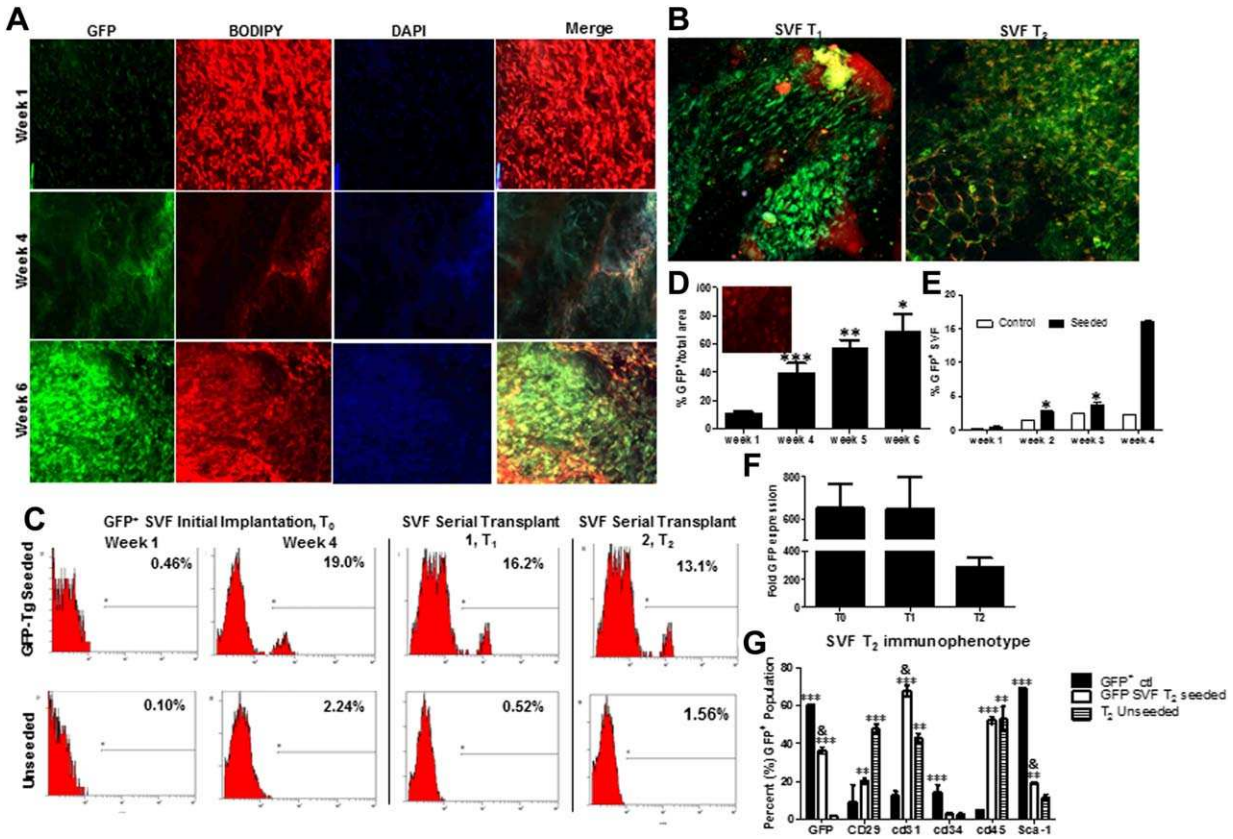

Figure 4. Detection of GFP-Tg SVF from tissue engineered adipose using HexaFluoroIsoPropanol 6-week silk scaffold implants in mice over two serial transplantations. Photomicrographs of GFP-Tg SVF cell implantation following weeks 1, 4, and 6 in vivo demonstrate persistence, proliferation, and ability to form GFP-Tg adipose depots. **(A)**: Confocal microscopy images of GFP, BODIPY, DAPI, and merged images within initial 6-week GFP-Tg SVF cell (T_0) transplants. **(B)**: Merged GFP/BODIPY/DAPI images of removed 6-week GFP-Tg SVF cell first serial (T_1) and second serial (T_2) transplants; sample size, $n = 5$. **(C)**: Flow cytometric analyses of GFP expression in removed adipose scaffolds following T_0, T_1, and T_2 transplants; sample size, $n = 18$. **(D)**: ImageJ analysis of weekly confocal images of T_0 explants. **(E)**: Quantification of weekly flow cytometric analyses of GFP expression in removed T_0 GFP-Tg SVF cell implants. **(F)**: GFP DNA expression in samples from removed 6-week T_0, T_1, and T_2 transplants. GFP expression reported as fold expression and normalized to GAPDH expression. **(G)**: Immunophenotype based on expression of GFP, CD29, CD31, CD34, CD45, and Sca-1 antigen expression on SVF cells isolated from 6-week T_2 transplants. Values reported as mean $\pm$ standard deviation ($\mu \pm SD$); comparing individual grouping to GFP^+ control: $^*p < .05$, $^{**}p < .01$; $^{***}p < .001$; comparing to GFP-SVF T_2 seeded to unseeded control groups: $^{\&}p < .05$. Abbreviations: GFP, green fluorescent protein; GFP-Tg, green fluorescent protein transgene; SVF, stromal vascular fraction.

difference was observed in glucose uptake between cohorts (Fig. 5H).

$CD146^-$ $CD34^+/CD29^+$ GFP-Tg ASC Detected Following Serial Transplantation

GFP-Tg ASC were detected within 6-week explants from initial cohorts (T_0 implants), as well as initial serial (T_1 implants; Fig. 6A). Tissue implants were infiltrated with blood vessels, which supports the earlier observation of tissue engraftment with GFP-Tg SVF and GFP-Tg ASC seeded scaffolds. Flow cytometry-based detection of freshly isolated GFP-Tg cells supported confocal microscopy observations of GFP positivity following week 6 of implantation (Fig. 6C, 6D). Initial CD34-enriched constructs resulted in detection of 29.4% GFP antigen positivity, compared to CD29-enriched constructs, which resulted in 10.9% GFP positivity via flow cytometry (Fig. 6C). CD34-enriched and CD29-enriched T_1 implants resulted in 20.4% and 8.4% GFP positivity, respectively (Fig. 6D). Quantification of GFP, BODIPY lipophilic dye, and DAPI colocalization staining was performed using ImageJ. GFP expression within explants was further investigated based on DNA and protein levels via qPCR and flow cytometry, respectively (Fig. 6E-6G). GFP DNA detected was 15-fold higher in CD34-enriched constructs compared to CD29-enriched constructs, and more than 10-fold higher than unsorted ASC constructs following T_1 implants (Fig. 6E). Detection of percent GFP-Tg cells via flow cytometry supported a significant difference in expression of GFP-Tg cells from CD34-enriched constructs compared to CD29-enriched constructs following 8 week T_0 implants (CD29, 9.8 ± 1.1; CD34, 24.7 ± 6.5; Fig. 6F) and T_1 implants (CD29, 5.4 ± 1.2; CD34, 17.5 ± 1.4; Fig. 6G).

$CD146^-$ $CD34^+$-Enriched Constructs Generate Functional GFP^+ Fat In Vivo

Adipose surrounding removed 8-week serial implants from GFP-Tg SVF seeded, unsorted GFP-Tg ASC, GFP-Tg CD34-enriched ASC, GFP-Tg CD29-enriched ASC, and GFP positive and negative controls, were removed and analyzed for GFP positivity (Fig. 7A-7C) and functionality (Fig. 7D, 7E). Confocal microscopy images of BODIPY stained removed adipose surrounding 8-week constructs revealed a significant increase in percent GFP-Tg adipocytes in CD34-enriched cohorts

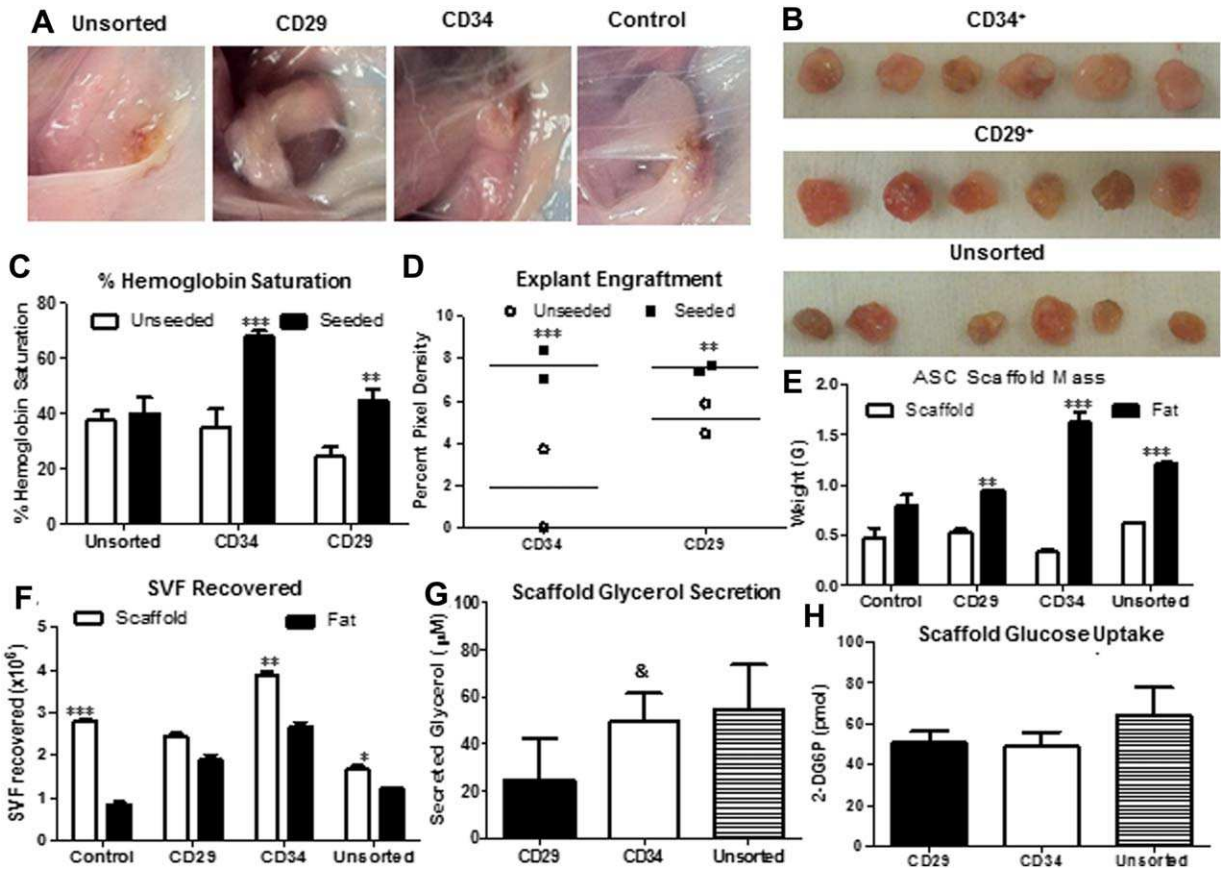

Figure 5. Adipose formation and functionality within green fluorescent protein transgene (GFP-Tg) ASC-seeded serial silk implants. **(A)**: Photomicrographs of scaffolds that were implanted with no cells (control), or with (a), 500k unsorted GFP-Tg ASC; (b), $CD146^{-}$ $CD29^{+}$ GFP-Tg ASC; or (c), $CD146^{-}$ $CD34^{+}$ GFP-Tg ASC; in silk scaffolds. Scaffolds were removed following 6 weeks of implantation. **(B)**: Images of removed scaffolds from cohorts (a)-(c). **(C)**: Percent hemoglobin saturation was measured in groups (a)-(c) after 6 weeks of initial (T_0) implantation. **(D)**: Quantification of removed scaffold (explant) engraftment via ImageJ analyses of photomicrographs in (B); sample size, $n = 6$ per grouping. **(E)**: Scaffold mass measurements after 6-week implants of cohorts (a)-(c), and control implants that were not seeded with any cells. **(F)**: Quantification of SVF recovered from 6-week implants, and surrounding fat from cohorts (a)-(c), and the unseeded control group; sample size, $n = 18$ per grouping. Functionality was measured via **(G)** glucose uptake, and (F) glycerol secretion assays using 6-week T_1 transplantation constructs. Data analyzed using Graphpad Prism. Two-way Analysis of Variances performed. Data reported as mean ± SD. $^{*}p < .05$, $^{**}p < .01$; $^{***}p < .001$; comparing to CD34-enriched group: $^{\&}p < .05$. Abbreviations: ASC, adipose stromal/stem cells; SVF, stromal vascular fraction.

compared to CD29-enriched, unsorted ASC, and SVF-seeded constructs (Fig. 7A, 7B). Quantification of images using ImageJ supported visual observations (SVF, 2.5 ± 1.7%; unsorted GFP-Tg ASC, 15.5 ± 0.2%; CD29-enriched, 6.1 ± 7.0%; CD34-enriched, 31.3 ± 0.4%; Fig. 7C). Further investigation of tissue engineered fat functionality revealed CD34-enriched constructs secreted glycerol levels comparable to unsorted ASC constructs whereas CD29-enriched constructs secreted significantly lower levels of glycerol (CD34, 70 ± 16.1 μM; unsorted ASC, 75 ± 22.1 μM; CD29, 40 ± 14.6 μM; Fig. 7D). Similar to removed constructs in Figure 5, no significant difference was observed in glucose uptake between cohorts (Fig. 7E).

Discussion

The present study transplanted freshly isolated GFP-Tg SVF cells using 3D silk matrices into non-GFP-Tg transgenic syngeneic murine hosts successfully over one initial, and two serial implants (2° implants). Initial time-based implant removal studies demonstrated GFP-Tg SVF cell survival, proliferation, and differentiation, leading to the formation of metabolically functional adipose tissue. Time-based GFP-Tg SVF experiments also revealed SVF cell ability to enhance engraftment and to reduce engraftment time. Expanded, plastic-adherent $CD146^{-}$ $CD29^{+}$ and $CD146^{-}$ $CD34^{+}$ P2 GFP-Tg ASC populations were seeded on 3D matrices, and implanted into non-GFP-Tg transgenic hosts successfully for an initial and serial implant (1° implants). To our knowledge, we are among the first to report the ability of specific subpopulations of nonpericytic ASC within the stromal vascular compartment to generate functional adipose over serial transplants.

These experiments were modeled after the serial transplant studies in the bone marrow literature which first validated the existence of HSCs [1]. The studies by Till et al. demonstrated that when hematopoietic cells were removed from the bone marrow and reinjected into γ-irradiated syngeneic recipient hosts, they would repopulate the bone marrow and restore basal hematopoietic activity [1, 36]. The present study supports the current literature suggesting that SVF cells

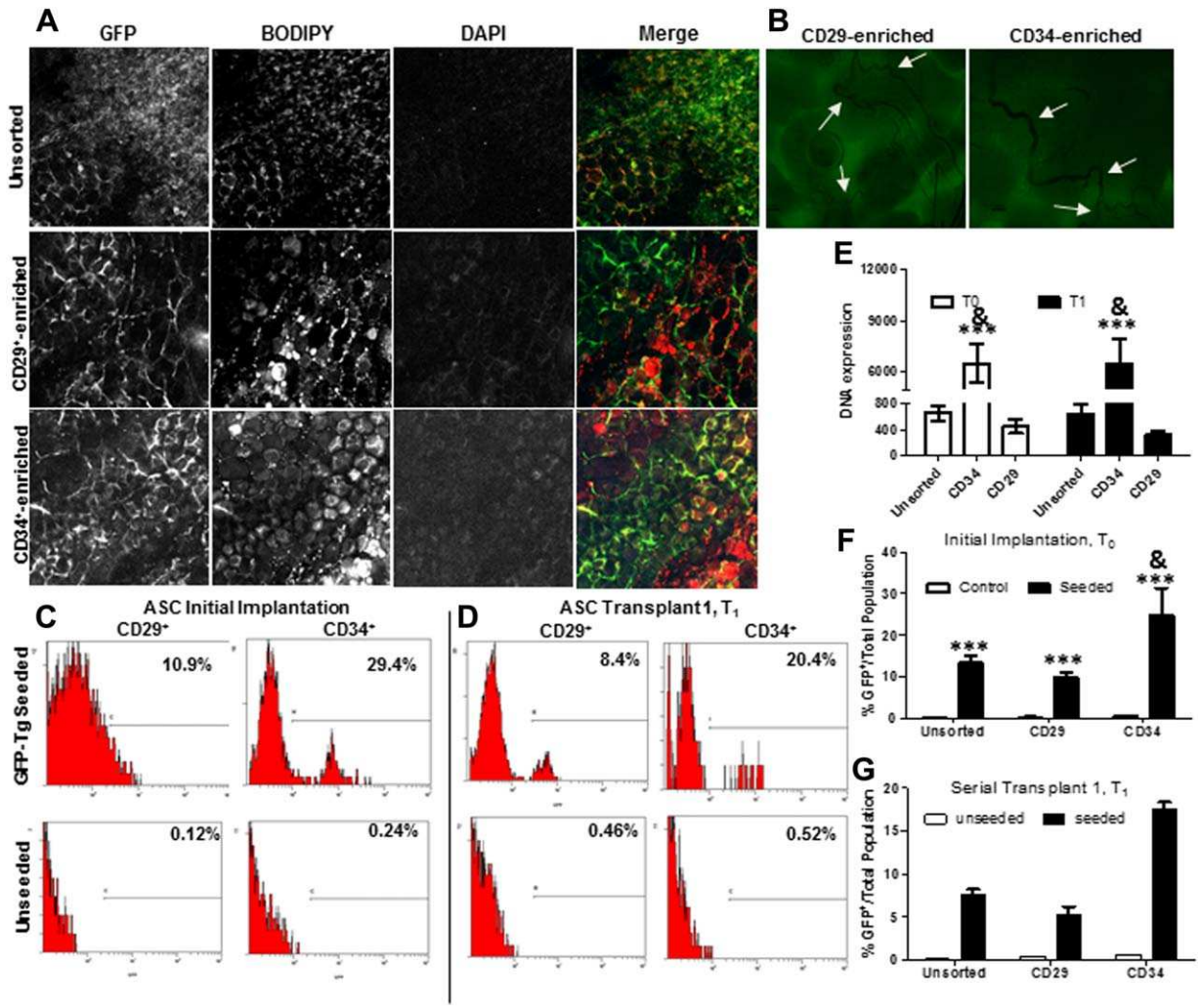

Figure 6. Detection of CD146$^-$ CD29$^+$ GFP-Tg ASC and CD146$^-$ CD34$^+$ GFP-Tg ASC from tissue engineered adipose using HexaFluoroIsoPropanol 6-week silk scaffold implants in mice over two serial transplantations. Photomicrographs of GFP-Tg CD29-enriched and CD34-enriched (cohorts (a)-(c) cell implantation following week 6 in vivo demonstrate persistence, proliferation, and ability to form GFP-Tg adipose depots, similar to unsorted GFP-Tg SVF cohorts. **(A)**: Confocal microscopy images of GFP, BODIPY, DAPI, and merged images from 6-week GFP-Tg ASC serial (T_1) transplants. **(B)**: Confocal images of CD29-enriched and CD34-enriched 6-week T_1 groups reflected observation of microvessel formation within CD34-enriched groups than in CD29-enriched groups; $n = 5$ per group per replicate. Flow cytometric analyses of GFP expression in removed adipose scaffolds from cohorts (a)-(c) following **(C)** T_0, and **(D)** T_1 transplants. **(E)**: GFP DNA expression in samples from removed 6-week T_0 and T_1 transplants. GFP expression reported as fold expression and normalized to GAPDH expression. Quantification of %GFP positivity following 6-week transplantation in **(F)** T_0 and **(G)** T_1 GFP-Tg ASC cell implants. Data reported as mean $\pm$ SD. Comparing individual grouping to unsorted cell seeded groups: $^*p < .05$, $^{**}p < .01$; $^{***}p < .001$; comparing to CD34-enriched group: $^{\&}p < .05$. Abbreviations: ASC, adipose stromal/stem cells; DAPI, GFP, green fluorescent protein; GFP-Tg, green fluorescent protein transgene; SVF, stromal vascular fraction.

and ASC have the ability to generate functional adipose tissues, and extends those observations to serial implantation of CD146$^-$ CD34$^+$-enriched GFP-Tg ASC, similar to the well-established HSC model [1, 34–38]. Mauney et al. reported on the ability of ASC to generate fat pads in rats using engineered scaffolds [35]. The objectives of their study included comparing biomaterials derived from silk fibroin prepared by aqueous (AB) and organic (HFIP) solvent-based processes, along with collagen and poly-lactic acid-based scaffolds, for their utility in adipose tissue engineering strategies. Their findings revealed HFIP silk-based matrices were superior to the other biomaterials and, therefore, suitable for other applications such as this study. This study, therefore, confirms and extends the findings by Mauney et al; however, the novelty is application of a more heterogeneous stromal vascular population, and usage in serial transplantation.

Due to the limitations of mouse tissue volume, ASC used in the present study were pooled from multiple mouse donors, and starting sample sizes for serial transplants were $n = 20$. A caveat within this study is the usage of CD34-enriched and CD29-enriched ASC populations that were expanded from freshly isolated mouse GFP-SVF; not CD34-exclusive and CD29-exclusive populations. Due to the rarity of CD29$^+$/CD34$^+$ double positive and CD29$^-$/CD34$^-$ double negative subpopulations within the freshly isolated SVF subfraction, the groupings in this study contained culture-expanded CD34$^+$ cells without consideration of CD29 coexpression. The same selection was used for CD29, without consideration of

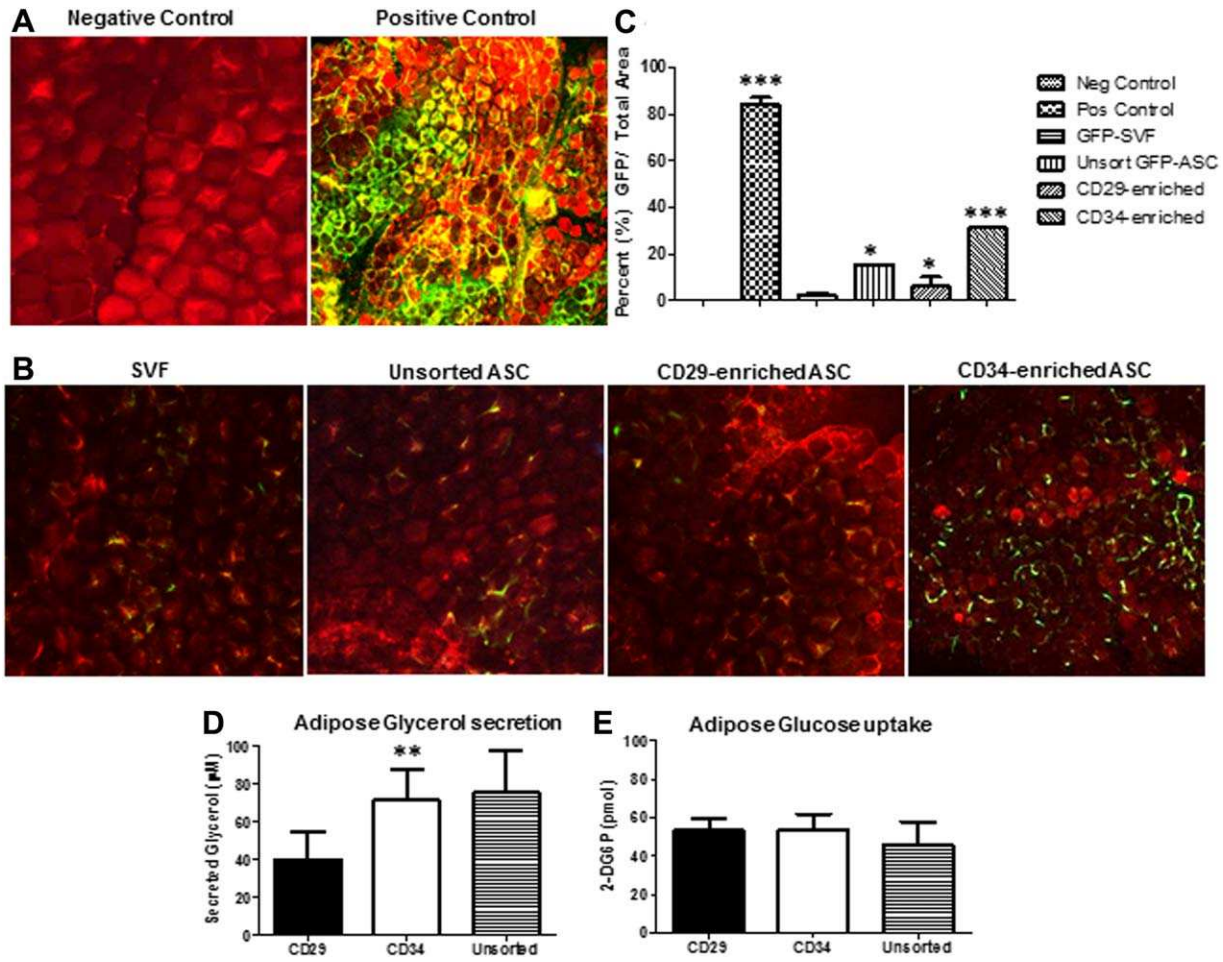

Figure 7. Green fluorescent protein transgene (GFP-Tg) SVF cells, CD29-enriched, and CD34-enriched GFP-Tg ASC infiltrate surrounding tissue to generate functional, GFP-Tg adipose. Confocal microscopic images of fat within 2 mm surrounding SVF and ASC constructs revealed GFP positivity. **(A)**:Merged images of negative and positive control adipose stained with BODIPY and DAPI in non-GFP-Tg mice and GFP-Tg mice, respectively. **(B)**: Images of adipose surrounding 6-week constructs that were seeded with unsorted GFP-Tg SVF cells, unsorted GFP-Tg ASC, and CD146$^-$ CD29-enriched and CD34-enriched GFP-Tg ASC; $n = 5$ per group per replicate. **(C)**: Quantification of confocal images from 7A and 7B. Functionality reported via **(D)** glycerol secretion, and **(E)** glucose uptake assays using 6-week T_1 transplantation constructs. Data reported as mean ± SD. *$p < .05$, **$p < .01$; ***$p < .001$. Abbreviations: ASC, adipose stromal/stem cells; GFP, green fluorescent protein; SVF, stromal vascular fraction.

CD34 coexpression. Therefore, a subpopulation within the CD34$^+$ GFP-ASC population also coexpressed CD29 and other cell surface and intracellular stromal markers that may be involved in anchorage, proliferation, migration, and adipogenic regulation. CD34$^+$ populations within freshly isolated murine SVF cells averaged 21.4% in the unsorted population; however, the CD34$^+$-enriched population in the SVF maintained an average of 33% positivity after two passages in culture. The percentage CD34$^+$ GFP-Tg ASC in this study are similar to published reports on CD34 positivity within human SVF [37]. The human CD34 positive populations were demonstrated to possess enhanced proliferative and adipogenic potential in vitro. A strong correlation was also identified between CD34$^+$ ASC yield and xenograft adipose tissue volume retention, suggesting that concentration of the CD34$^+$ progenitor can predict human fat graft survival in clinical settings [37–40]. Future experiments will extend the study to a more humanized system, initially by examining the behavior of sorted human cells in an immunodeficient murine model. These experiments will also allow for larger initial sample sizes that are greater than $n = 20$, and may lead to serial transplantation beyond secondary transplants (3° and beyond).

The current literature refers to cells that aid in fat grafting survival using the terms, "adipose stromal" cell and "perivascular stem" cell interchangeably. Traditionally, perivascular stem cells are identified based on an immunophenotype of CD45$^-$, CD146$^+$, and CD34$^-$ [40]. The results from CD146$^-$ CD34$^+$-enriched ASC serial implants indicate the presence of a nonpericytic ASC subpopulation within SVF that is capable of generating functional fat pads in mice over successive transplants. These findings are supported by in vivo cell fate/mapping studies where tissue resident stem cells in neonatal mice were labeled with bromo-deoxyuridine (BrdU) [41]. Eight weeks later, histological analyses of inguinal adipose depots determined that the BrdU label retaining stem cells could be found in the perivascular space (consistent with a pericytic subpopulation) and at a substantial distance from the capillaries, in the vicinity of mature adipocytes (consistent with a

nonpericytic population) [41]. Although the $CD146^-$ population represents the majority of the plastic-adherent population (80%) in this study, only 20% of these cells coexpress the progenitor cell antigen CD34. Nevertheless, the current results indicate that nonpericytic cells can serve as adipogenic stem cells in vivo.

Confocal fluorescence imaging measurements of %Hb saturation at weeks 1 and 4 demonstrated that the presence of GFP-Tg SVF or enriched GFP-Tg ASC accelerated scaffold engraftment as early as week 1 of implantation. Measurements of the SVF recovered from the explants and scaffold weights at weeks 1 and 2 supported these data. Current published reports suggest SVF and ASC encourage the enhancement of engraftment and acceleration of wound healing in a variety of applications, including both soft and hard tissue remodeling, and for the improvement of pathophysiological conditions [42]. Mesimaki et al. demonstrated the usage of expanded ASC for the enhancement of a maxillary flap with β-tricalcium phosphate and bone morphogenetic protein 2 (BMP2). Addition of the expanded ASC aided in the development of mature bone structures and vasculature [43]. Yoshimura et al. reported high surgeon and patient satisfaction 12 months postoperatively in 55 patients receiving adipose tissue grafts augmented with SVF cells, a procedure termed "cell-assisted lipotransfer (CAL)," instead of prosthetic breast enhancement [44]. More recently, Bura et al. have employed autologous human ASC to treat patients with critical ischemic limbs and have observed significant improvements in tissue oxygen delivery [29]. Together, these human clinical studies lend credence to the findings in our murine preclinical model.

Confocal microscopy and flow cytometric analyses of 8-week serial implants indicated that $CD34^+$-enriched subpopulations are capable of generating functional fat pads, similar to unsorted ASC implants. $CD34^+$-enriched ASC were demonstrated to proliferate and undergo adipogenic differentiation at higher rates than $CD29^+$-enriched and unsorted ASC in vitro. In vivo, higher percentages of SVF cells were recovered from CD34-enriched constructs. These explants averaged higher scaffold masses than CD29-enriched and unsorted ASC cohorts. Functional analyses of fat surrounding the scaffolds after 6 weeks revealed CD34-enriched explants exhibited higher glycerol secretion than CD29-enriched, unsorted ASC, and control unseeded implants. GFP-Tg SVF and -ASC were detected within surrounding adipose depots. BODIPY staining, glycerol uptake, and lipolysis analyses suggest these cells may have been proliferating, differentiating within the scaffold, and migrating locally as mature adipocytes or as preadipocytes. These data suggest that a subpopulation phenotypically found within the $CD146^-$ $CD34^+$-enriched ASC population is capable of generating functional fat pads over serial passages. These findings are consistent with studies by Philips et al. demonstrating that the functionality and volume retention of human adipose tissue xenografts correlated with the frequency of $CD34^+$ cells in the donor tissue [37].

Conclusion

It remains challenging to distinguish cell categories between "stromal/progenitor" and "stem" cell. Nevertheless, the current serial transplant findings suggest that the inguinal WAT of adult mice contains a flow cytometry, sortable subpopulation of cells capable of contributing to the regeneration and serial transplantation of a functional adipose tissue depot. These findings confirm and extend earlier studies by Rodeheffer et al. examining the ability of flow cytometry sorted adipose-derived cells to regenerate adipose depots in lipodystrophic mice [2, 45]. Additionally, these outcomes further validate the utility of autologous adipose-derived cells for functional tissue engineering [46]. The work also extends prior studies characterizing the immunophenotype and pericyctic properties of isolated adipocyte progenitor cells [47–49].

Acknowledgement

This work was funded in part by funding from the National Institutes of Health (R21DK094254).

Authors Contributions

All coauthors have contributed significantly to the production of this manuscript. A.B., A.S., and S.L. were instrumental in executing planned experiments. R.A. and D.K. graciously provided synthesized HFIP-based silk scaffolds for cell seeding and serial transplantation studies. H.T. performed flow cytometry and fluorescence-activated cell sorting experiments within the flow cytometry core facility. M.W. and Q.B.: provided access to Zenalux Zenascope instrumentation, training, and access to raw data for hemoglobin comparison analyses within cohorts. J.H. performed cryo-SEM studies. T.F. performed all other experiments within the study and drafted the manuscript. B.A.B. and J.G. both developed the aims of the studies and were instrumental in finalization of the manuscript. All coauthors read and approved the final manuscript.

Potential Conflicts of Interest

J.M.G. is the co-owner, cofounder, and Chief Scientific Officer of LaCell LLC, a biotechnology company focusing research and clinical translation of adipose-derived stromal/stem cells. J.Q.B. has financial interest and serves as a consultant for Zenalux Biomedical, Inc., a manufacturer of the quantitative tissue optical spectrometer used in this work.

Note Added in Proof

While this manuscript was under review, Hu et al. (2015) reported that IGF1 enriched for a subpopulation of $CD31^-$/$CD34^+$/$CD146^-$ cells in human adipose tissue that were robustly adipogenic. The current manuscript in a murine model complements the Mao laboratory's previously reported mechanistic findings.

Hu L, Yang G, Hägg D, Sun G, Ahn JM, Jiang N, Ricupero CL, Wu J, Rodhe CH, Ascherman JA, Chen L, Mao JJ. IGF1 Promotes Adipogenesis by a Lineage Bias of Endogenous Adipose Stem/Progenitor Cells. Stem Cells. 2015 Aug;33(8):2483–2495.

References

1 Till JE, McCulloch EA, Siminovitch L. A stochastic model of stem cell proliferation, based on the growth of spleen colony-forming cells. Proc Natl Acad Sci USA 1964; 51:29–36.

2 Ramalho-Santos M, Willenbring H. On the origin of the term "stem cell". Cell Stem Cell 2007;1:35–38.

3 Zuk PA, Zhu M, Ashjian P et al. Human adipose tissue is a source of multipotent stem cells. Mol Biol Cell 2002;13:4279–4295.

4 Guilak F, Lott KE, Awad HA et al. Clonal analysis of the differentiation potential of human adipose derived adult stem cells. J Cell Physiol 2006;206:229–237.

5 Izadpanah R, Trygg C, Patel B et al. Biologic properties of mesenchymal stem cells derived from bone marrow and adipose tissue. J Cell Biochem 2006;99:1285–1297.

6 Maumus M, Peyrafitte JA, D'Angelo R et al. Native human adipose stromal cells: Localization, morphology, and phenotype. Int J Obesity (London) 2011;9:1141–1153.

7 Kim JH, Jee MK, Lee SY et al. Regulation of adipose tissue stromal cells behaviors by endogenic Oct4 expression control. PloS One 2009;4:e7166.

8 Crossno JT, Majka SM, Grazia T et al. Rosiglitazone promotes development of a novel adipocyte population from bone marrow-derived circulating progenitor cells. J Clin Invest 2006;116:3220–3228.

9 Koh YJ, Kang S, Lee HJ et al. Bone marrow-derived circulating progenitor cells fail to transdifferentiate into adipocytes in adult adipose tissues in mice. J Clin Invest 2007;117:3684–3695.

10 Majka SM, Fox KE, Psilas JC et al. De novo generation of white adipocytes from the myeloid lineage via mesenchymal intermediates is age, adipose depot, and gender specific. J Clin Invest 2010;107:14781–14786.

11 Zannetinno AC, Paton S, Arthur A et al. Multipotential human adipose-derived stromal stem cells exhibit a perivascular phenotype in vitro and in vivo. J Cell Physiol 2008; 214:413–421.

12 Crisan M, Yap S, Casteilla L et al. A perivascular origin for mesenchymal stem cells in multiple human organs. Cell Stem Cell 2008; 3:301–313.

13 Traktuev DO, Merfeld-Clauss S, Li J et al. A population of multipotent CD34-positive adipose stromal cells share pericyte and mesenchymal surface markers, reside in a periendothelial location, and stabilize endothelial networks. Circ Res 2008;102:77–85.

14 Gimble JM, Katz AJ, Bunnell BA. Adipose-derived stem cells for regenerative medicine. Circ Res 2007;100:1249–1260.

15 Yoshimura K, Sato K, Aoi N et al. Cell-assisted lipotransfer for facial lipoatrophy: Efficacy of clinical use of adipose-derived stem cells. Dermatol Res 2009;34:1178–1185.

16 Yoshimura K, Asano Y, Aoi N et al. Breast J 2010;16:169–175.

17 Rubin JP, Marra KG. Soft tissue reconstruction. Progenitor-enriched adipose tissue transplantation as rescue for breast implant complications. Methods Mol Biol 2011;702: 395–400.

18 Maggini J, Mirkin G, Bognanni I et al. Mouse bone marrow-derived mesenchymal stromal cells turn activated macrophages into a regulatory-like profile. PloS One 2010;5: e9252.

19 Al-Zoubin M, Salem AF, Martinez-Outschoorn UE et al. Creating a tumor-resistant microenvironment: Cell-mediated delivery of TNFα completely prevents breast cancer tumor formation in vivo. Cell Cycle 2013;12:480–490.

20 Li P, Sun H, Du M et al. Adult rat hippocampus soluble factors: a novel transplantation model mimicking intracranial microenvironment for tracing the induction and differentiation of adipose-derived stromal cells in vitro. Neurosci Lett 2013;542:5–11.

21 Mazo M, Planat-Bénard V, Abizanda G et al. Transplantation of adipose derived stromal cells is associated with functional improvement in a rat model of chronic myocardial infarction. Eur J Heart Fail 2008;10: 454–462.

22 Cai L, Johnstone BH, Cook TG et al. IFATS collection: Human adipose tissue-derived stem cells induce angiogenesis and nerve sprouting following myocardial infarction, in conjunction with potent preservation of cardiac function. Stem Cells 2009;27:230–237.

23 Schenke-Layland K, MacLellan WR. Induced pluripotent stem cells: It's like déjà vu all over again. Circulation 2009;120:1462–1464.

24 Kang SK, Lee S, Oh HK et al. Clinical features of deep neck infections and predisposing factors for mediastinal extension. Korean J Thorac Cardiovasc Surg 2012;45:171–176.

25 Kim JM, Lee ST, Chu K et al. Systemic transplantation of human adipose stem cells attenuated cerebral inflammation and degeneration in a hemorrhagic stroke model. Brain Res 2007;1183:43–50.

26 Ikegame Y, Yamashita K, Hayashi S et al. Comparison of mesenchymal stem cells from adipose tissue and bone marrow for ischemic stroke therapy. Cytotherapy 2011;13:675–685.

27 Rehman J, Traktuev D, Li J et al. Secretion of angiogenic and antiapoptotic factors by human adipose stromal cells. Circulation 2004;109:1292–1298.

28 Planat-Benard V, Silvestre JS, Cousin B et al. Plasticity of human adipose lineage cells toward endothelial cells: Physiological and therapeutic perspectives. Circulation 2004;109:656–663.

29 Moon MH, Kim SY, Kim YJ et al. Human adipose tissue-derived mesenchymal stem cells improve postnatal neovascularization in a mouse model of hindlimb ischemia. Cell Physiol Biochem 2006;17:279–290.

30 Bura A, Planat-Benard V, Bourin P et al. Phase I trial: The use of autologous cultured adipose-derived stromal/stem cells to treat patients with non-revascularizable critical limb ischemia. Cytotherapy 2014;16:245–257.

31 Yu G, Wu X, Kilroy G et al. Isolation of murine adipose-derived stem cells. Methods Mol Biol 2011;702:29–36.

32 Mitchell JB, McIntosh K, Zvonic S et al. The immunophenotype of human adipose derived cells: Temporal changes in stromal and stem cell-associated markers. Stem Cells 2006;24:376–385.

33 Zimmerlin L, Donnenberg VS, Rubin JP et al. Mesenchymal markers on human adipose stem/progenitor cells. Cytometry A 2013;83:134–140.

34 Barnes DW, Ford CE, Loutit JF. Serial grafts of homologous bone marrow in irradiated mice. Sang 1959;30:762–765.

35 Mauney JR, Nguyen T, Gillen K et al. Engineering adipose-like tissue in vitro and in vivo utilizing human bone marrow and adipose-derived mesenchymal stem cells with silk fibroin 3D scaffolds. Biomaterials 2007;28:5280–5290.

36 Vos O, Dolmans MJ. Self-renewal of colony forming units (CFU) in serial bone marrow transplantation experiments. Cell Tissue Kinet 1972;5:371–385.

37 Philips BJ, Grahovac TL, Valentin JE et al. Prevalence of endogenous CD34 + adipose stem cells predicts human fat graft retention in a xenograft model. Plast Reconstr Surg 2013;132:845–858.

38 Yoshimura K, Eto H, Kato H et al. In vivo manipulation of stem cells for adipose tissue repair/reconstruction. Regen Med 2011;6: 33–41.

39 Yoshimura K, Sato K, Aoi N et al. Cell-assisted lipotransfer for cosmetic breast augmentation: Supportive use of adipose-derived stem/stromal cells. Aesthetic Plast Surg 2008;32:48–55; discussion 56–47.

40 Li H, Zimmerlin L, Marra KG et al. Adipogenic potential of adipose stem cell subpopulations. Plast Reconstr Surg 2011;128: 663–672.

41 Gawronska-Kozak B, Staszkiewicz J, Gimble JM et al. Recruitment of fat cell precursors during high fat diet in C57BL/6J mice is fat depot specific. Obesity 2014;22:1091–1102.

42 Kokai LE, Marra K, Rubin JP. Adipose stem cells: Biology and clinical applications for tissue repair and regeneration. Transl Res 2014;163:399–408.

43 Mesimaki K, Lindroos B, Tornwall J et al. Novel maxillary reconstruction with ectopic bone formation by GMP adipose stem cells. Int J Oral Maxillofac Surg 2009; 38:201–209.

44 Yoshimura K, Asano Y, Aoi N et al. Cell-assisted lipotransfer for cosmetic breast augmentation: Supportive use of adipose-derived stem/stromal cells. Aesthet Plast Surg 2008;32:48–57.

45 Rodeheffer MS, Birsoy K, Friedman JM. Identification of white adipocyte progenitor cells in vivo. Cell 2008;135:240–249.

46 Hu L, Yang G, Hägg D et al. IGF1 promotes adipogenesis by a lineage bias of

endogenous adipose stem/progenitor cells. Stem Cells 2015;33:2483–2495.

47 Hebert TL, Wu X, Yu G et al. Culture effects of epidermal growth factor (EGF) and basic fibroblast growth factor (bFGF) on cryopreserved human adipose-derived stromal/stem cell proliferation and adipogenesis. J Tissue Eng Regen Med 2009;3:553–561.

48 James AW, Zara JN, Corselli M et al. An abundant perivascular source of stem cells for bone tissue engineering. Stem Cells Transl Med 2012;1:673–684.

49 Berry R, Rodeheffer MS. Characterization of the adipocyte cellular lineage in vivo. Nat Cell Biol 2013;15:302–308.

See www.StemCells.com for supporting information available online.